COMPDYN 2013
4th ECCOMAS Thematic Conference on
Computational Methods in Structural Dynamics and Earthquake Engineering
M. Papadrakakis, V. Papadopoulos, V. Plevris (eds.)
Kos Island, Greece, 12–14 June 2013

OPTIMUM SELECTION OF RETROFIT MEASURES FOR R/C BRIDGES USING FRAGILITY CURVES

Sotiria P. Stefanidou[1], **Andreas J. Kappos**[2]

[1] Department of Civil Engineering, Aristotle University of Thessaloniki
54124 Thessaloniki, Greece
e-mail: ssotiria@civil.auth.gr

[2] Department of Civil Engineering, City University London
London EC1V OHB, UK
Andreas.Kappos.1@city.ac.uk

Keywords: Bridge Retrofit, Pier Jackets, Bearing Replacement, Global and Local Engineering Demand Parameters, Fragility curves

Abstract. *The key objective of this paper is to present a methodology for the selection of the appropriate retrofit scheme for bridges, based on the performance of different components (piers, bearings, abutments) with a view to upgrading the seismic performance of the system. The methodology is applied to a common bridge type, with monolithic pier-to-deck connections. Threshold values for global and local parameters are properly defined based on performance criteria, for different damage states. The correlation of local and global threshold values calculated on the basis of member and system capacity, respectively, reveals the structural system's robustness and identifies the most critical member with respect to the seismic performance of the system. Alternative retrofit measures, i.e. reinforced concrete (R/C) and fibre-reinforced polymer (FRP) jackets, and bearing replacement, are applied to critical members of the structure.*

Fragility curves are generated for the resulting retrofitted bridges using a probabilistic seismic demand model based on the results of inelastic dynamic response history analysis for appropriately selected earthquake ground motions, while bridge capacity is estimated through pushover analysis. The engineering demand parameter used for the quantification of the limit state threshold values for the retrofitted bridge is the bridge displacement (global parameter), related to the most critical component's displacement for every limit state and to local parameters (such as the pier curvature ductility). Alternative sets of retrofit properties are considered, and material uncertainties are treated in a probabilistic way in the bridge model (Latin Hypercube Sampling Method). The alternative retrofit schemes are finally evaluated and the optimum retrofit solution is identified on the basis of its efficiency, emerging from the comparison of fragility curves (as-built and retrofitted case) for different levels of seismic action.

1 INTRODUCTION

Damage due to recent earthquakes worldwide, albeit minor in several cases, highlights the role of bridges as the most vulnerable component of the transportation network. Bridge damage (Fig. 1) can cause significant disruption to the transportation system, resulting in substantial direct and indirect losses. The Loma Prieta 1989 earthquake resulting in more than 40 deaths due to bridge damage and $1.8 billion direct losses due to damage to the transportation system [1] has shown the need for retrofit of older bridges in order to reduce their vulnerability and withstand a future seismic event with controlled damage. Retrofit measures used for the enhancement of the bridges' seismic performance were tested during the 1994 Northridge earthquake, where significant damage occurred to older as well as retrofitted bridges, resulting in questioning the effectiveness of several retrofit measures and strategies used.

Figure 1: Bridge damage due to recent earthquakes.

Pre-earthquake retrofit decision making should best be based on the results of probabilistic assessment of the bridges' seismic performance for different levels of seismic hazard. The use of fragility curves for assessing the vulnerability of bridges became a common practice during the last two decades. Numerous methodologies for the derivation of empirical [2], as well as analytical fragility curves [3,4,5,6,7,8,9] have been developed. The differences among the existing methodologies mainly lie in the quantitative definition of limit states (engineering demand parameter used, threshold values of limit states considered), the type of analysis, and the probabilistic model used for the fragility analysis. The probability of reaching or exceeding a specific limit state is calculated on the basis of exceeding threshold values of an engineering demand parameter, correlated to damage in the system. The engineering demand parameter may be either a global parameter (bridge displacement) [5,8] or a local one (material strains, column ductility, bearing deformation) [3,4,9], whereas the damage index is also commonly used [6]. The bridge fragility may be defined considering one bridge component as the most critical for the bridges' seismic performance [6,7] or a combination of different bridge components [3,4,10] in a series or parallel system [10,11].

Recent methodologies [3,4,5,9] propose the combination of component fragility curves for the derivation of the system fragility. Bridge piers, abutments, and bearings are considered to be the most critical components regarding the bridge seismic performance. The probabilities of the demand exceeding the capacity are calculated separately for each component and every limit state, based on local engineering demand parameters, and the derived component fragilities are subsequently synthesised in order to derive the overall system's fragility.

Since fragility curves can be used for retrofit prioritization and decision-making, system fragility should preferably highlight the most vulnerable component for every limit state, so that it can guide the designer to the most effective intervention for the enhancement of the system's performance to the desired level. The latter requires mapping between component (local) and system (global) capacities for the limit state definition and only recently [12] the research interest moved towards this direction.

Retrofit measures for the enhancement of bridge seismic performance can be categorized into those that target strength, stiffness, or ductility, enhancement (R/C, steel, or FRP pier jackets), the increase of energy dissipation (elastomeric or lead bearings, isolation systems), or control of displacements (restrainer cables, shear keys, seat extenders). Steel and FRP jackets are arguably the most popular retrofit measures for bridge piers [13,14], since they increase the flexural and shear strength as well as the member's ductility without significant change to the member stiffness that will typically result to increased seismic forces. The behaviour of FRP jackets has been investigated experimentally as well as analytically [15,16]; nevertheless, their implementation requires qualified staff that might not be locally available, as FRPs are not as widely used as R/C jackets. Replacement of existing bearings with elastomeric and lead rubber bearings, and addition of energy dissipation devices were found to be very effective for the pre-earthquake retrofit since they reduce the seismic input to the structure [17]. Their effectiveness has been evaluated and optimum properties for the system's vulnerability reduction have been defined [11]. Finally, various retrofit measures concerning the structure's displacement control (including unseating), namely restrainer cables, shape memory alloys, shear keys and seat extenders were evaluated experimentally as well as analytically with regard to both component and system vulnerability reduction [18].

Figure 2: Retrofit measures for R/C bridges.

The most efficient retrofit measures and retrofit strategies for the enhancement of the bridge seismic performance are not always apparent, and use of advanced computational tools is necessary for their proper selection and comparative evaluation. Fragility curves of retrofitted bridges quantify the efficiency of retrofit measures, when compared to the as-built ones. Limited studies concerning various retrofit measures applied to a single bridge component [19,20] or a number of components [10] reveal the retrofit impact and the performance of the retrofitted structures under various seismic intensities. Another important issue apart from the efficiency of the retrofit measures is the efficiency of retrofit strategies [1] that can emerge from the combination of different retrofit measures applied to the system components.

The key objective of this paper is the presentation of a methodology for the derivation of fragility curves using a component-level approach, relating the component (local) to system (global) limit state capacities (threshold values for each limit state) in order to identify the most critical component for each limit state. A parametric study is carried out to assess the sensitivity of the system capacity to different geometric, reinforcement, and soil-foundation

properties of the components. To enhance the seismic performance, different retrofit measures might be appropriate for different performance levels; R/C and FRP pier jackets as well as bearing replacement, are evaluated here through fragility analysis of the retrofitted bridges and the optimum selection of retrofit measure is discussed.

2 METHODOLOGY FOR THE DERIVATION OF FRAGILITY CURVES CORRELATING COMPONENT TO SYSTEM PERFORMANCE

A new methodology for the derivation of bridge fragility curves is presented, focusing on the correlation between system (global) and component (local) seismic performance and associated guidelines for the most effective retrofit intervention for the selected performance level(s). The methodology consists of three distinct steps and is described in the next sections.

2.1 Component Subsystems – Correlation between local and global engineering demand parameters for the definition of limit state threshold values

A critical issue for the derivation of fragility curves is the definition of limit states. Limit states are typically related to damage observed to the structural system or member by means of an engineering demand parameter, which can either refer to the whole system (displacement) [5,8] or to a bridge member [7] or section [4,21]. Threshold values of engineering demand parameters reflect the bounds of the system's capacity for each limit state.

The first step of the proposed methodology refers to the definition of subsystems, critical for the seismic performance of the bridge system. Bridge piers, abutments and bearings were found to be the most important bridge components as far as performance under seismic actions is concerned [4,9,10,11]. The importance of the foundation is also recognized, though it is not considered as a different subsystem at this stage of development of the method.

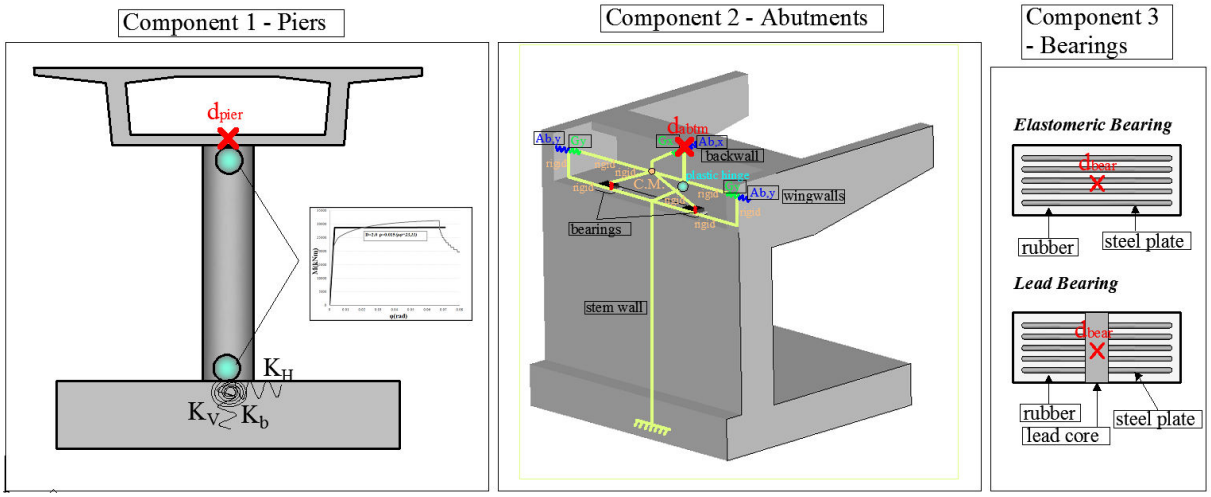

Figure 3: Subsystems consisting of bridge critical components.

According to the proposed methodology the aforementioned subsystems are individually analysed. Boundary conditions are introduced through equivalent translational and rotational springs at connection points with the deck, calculated through static condensation of the full model, while equivalent mass is also estimated and introduced. Foundation translational and rotational springs are defined here for the case of shallow foundation. Threshold values for engineering demand parameters are defined based on local parameters and are correlated to global ones (component control point displacement) with the aid of pushover analysis.

The bridge piers considered are monolithically connected to the deck, hence having two potential plastic hinge formation regions located at the top and bottom of the pier. The piers are modelled using beam-column elements with concentrated plastic hinges at the top and bottom. Cross section analysis is performed [23] using appropriate stress-strain curves for concrete and steel [24] in order to obtain moment-curvature diagrams, while the plastic hinge length L_p is also calculated [25]. The engineering demand parameter used for the definition of limit states threshold values is the curvature (Table 1), related to material strain limits [25,26] that correspond to experimentally observed member damage (cover spalling, buckling of longitudinal reinforcement, first hoop fracture) and crack widths [26]. It is noted that in the present study only flexural failure modes are taken under consideration.

Limit State	Threshold values of curvature (φ)	Quantitative Performance Description
LS 1 – Minor/Slight damage	φ_y	Quasi-elastic behaviour – Cracks barely visible.
LS 2 – Moderate damage	min (φ: $\varepsilon_c \leq 0.004$, φ: $\varepsilon_s \geq 0.015$)	Spalling of the cover concrete , strength may continue to increase – Crack width 1-2mm.
LS 3 – Major/Extensive damage	min (φ: $\varepsilon_c \leq 0.004 + 1.4\rho_w \cdot \frac{f_{yw}}{f_{cc}}$, φ: $\varepsilon_s \geq 0.06$)	First hoop fracture, buckling of longitudinal reinforcement, initiation of crushing of concrete core – Crack width>2mm.
LS 4 – Failure/Collapse	min (φ: $M_{res} < 0.85 \cdot M_{max}$ φ: $\varepsilon_s \geq 0.075$)	Loss of load-carrying capacity - Collapse

Table 1: Limit states for component 1: Bridge Piers.

For the threshold values of limit states to be quantified, inelastic static pushover analysis is performed to the subsystem and the component's control point displacement corresponding to each threshold local engineering demand parameter (φ) value is monitored. Hence, limit states in terms of deformation (global parameter) are directly mapped to limit states in terms of curvature (local parameter) for the component under consideration.

Limit State	Threshold values	Quantitative Performance Description
LS 1 – Minor/Slight damage	$\mu_{\varphi,backwall}$=1.5	Cracking and significant damage to the backwall
LS 2 – Moderate damage	$d = 0.01 \cdot h_{backwall}$	First yield of the abutment soil
LS 3 – Major/Extensive damage	$d = 0.035 \cdot h_{backwall}$	Excessive deformation of abutment soil
LS 4 – Failure/Collapse	$d = 0.1 \cdot h_{backwall}$	Ultimate deformation of abutment soil (cohessionless soil)

Table 2: Limit states for component 2: Abutments.

Limit state threshold displacement values are defined in a similar way for the abutment. The abutment was modelled using beam column elements with potential hinges in the backwall as shown in Figure 3. Cross section analysis was performed for the backwall [23] in or-

der to obtain moment-curvature diagrams, and the plastic hinge length L_p is calculated as before [25]. The embankment-abutment interaction (passive action) after gap closure was considered [22] taking under consideration the Caltrans provisions. Limit state definitions for the abutments are given in Table 2. Subsequently, inelastic static (pushover) analysis is performed for the abutment subsystem in order to define the threshold value in terms of displacement of the control point for the first limit state (the other three LSs are directly expressed in terms of fractions of the backwall height).

Except from the piers and abutments another critical bridge component, namely the bearings, is considered. The bearing stiffness is properly defined [27] and modelled using an elastoplastic hysteresis model. The engineering demand parameter used to define the component's threshold limit state values is the shear strain (γ=d/t,$_{rubber}$) [28]; threshold values based on information from the literature are given in Table 3.

Limit State	Threshold values of shear strain (γ)	Quantitative Performance Description
LS 1 – Minor/Slight damage	100%	Initiation of nonlinear behaviour, potential yielding of anchor bolts and cracking of pedestals.
LS 2 – Moderate damage	150%	Visible damage to the bearing. Yield of steel shims.
LS 3 – Major/Extensive damage	200%	Lift off at the edge of the bearing, uplift and rocking. May cause delamination, bonding failure between rubber layers and steel shim plates.
LS 4 – Failure/Collapse	250%	Lift-off, rotation. Unseating, failure of bearings.

Table 3: Limit states for component 3: Bearings.

2.2 Bridge system capacity – Definition of limit states for the system in terms of global parameters

Since the combination of components may influence the seismic performance of the system differently, formulation of the whole system bridge model is necessary to relate the bridge control point displacement to the displacement of the control (monitoring) point of individual components and define the threshold limit state values (capacity) for the system.

Pushover analysis of the bridge system is performed for the longitudinal and transverse direction. Displacement of the control point is recorded when each one of the components considered enters a specific limit state as depicted in Figure 4; the bridge centre of mass is taken as the control point for the longitudinal direction, whereas the bridge end is taken for the transverse direction, since in the studied bridge this is the point of maximum displacement. The threshold value for the limit state considered is taken as the minimum of the displacements obtained, assuming a series connection between the components (conservative approach). Therefore the threshold values for every limit state are defined for the system in terms of the displacement of the control point (global parameter), hence being directly correlated to local performance of the components.

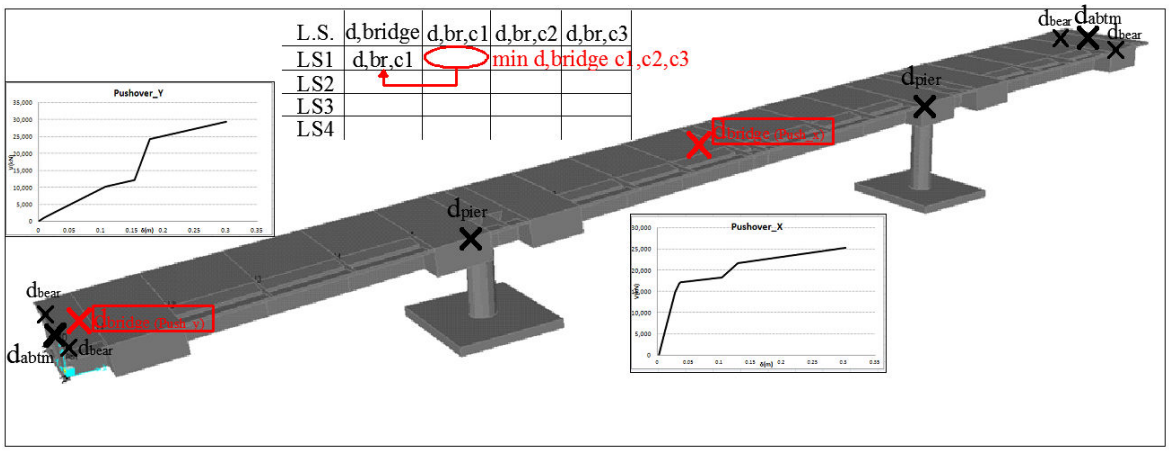

Figure 4: Bridge system limit state definition.

2.3 Uncertainties in capacity and demand

Aleatory and epistemic uncertainties should be considered during the demand and capacity estimation regarding the material and geometric properties, whereas other type of uncertainties, such as the uncertainty in the limit state definition are also deemed to be important.

Different bridge realizations, statistically different, yet nominally identical, are considered for the probabilistic treatment of fragility curves and Latin Hypercube sampling (LHS) is implemented to reduce the computational effort. LHS is as a stratified sampling procedure, that provides an efficient way of sampling variables from their distributions while limiting the required sample size compared to Monte Carlo sampling methods. The algorithm suggested by Iman and Conover [29] was implemented in the frames of the proposed methodology for the treatment of uncertainty in capacity and demand .

2.4 Fragility Curves

Fragility curves represent the conditional probability of reaching or exceeding a limit state as a function of a ground motion intensity parameter.

$$P_F = P[D \geq C] \tag{1}$$

where P_F= probability of failure, D=structural demand and C=structural capacity. Various intensity measures (PGA, S_a, S_v) were evaluated based on their efficiency, practicality, sufficiency and hazard computability, with the PGA considered as the optimum choice for the derivation of fragility curves [18].

Having defined the capacity of the bridge from step 2, the Probabilistic Seismic Demand Model (PSDM) is employed to derive analytical fragility functions using nonlinear response history analysis of the bridge. There are two approaches regarding the implementation of the PSDM, namely the “cloud” (Probabilistic Seismic Demand Analysis) and the “scaling” (Incremental Dynamic Analysis) approach, with the latter having the advantage of not requiring an a priori assumption for the probabilistic distribution of seismic demands in order to derive fragility curves [11].

The one implemented herein is the IDA approach for different levels of seismic action ranging from 0.4 to 4 times the A_d. The limit state probability of exceedance at a specific IM level equals the occurrence ratio of the specific limit state, defined as the ratio of the number of damage cases n_i, for the damage state I over the number of simulations *N*, as noted in equation 2.

$$P[\langle D \geq DS_i | I_M \rangle = \frac{n_i}{N} \quad (i = 1 \; to \; 4) \tag{2}$$

Fragility curves are commonly fitted with a log-normal cumulative distribution function [8,11] (equation 3) and if normalized to A_d become independent of the design seismic action [30].

$$P[\langle DI \geq LS | I_M \rangle = \int_{-\infty}^{I_M} \frac{1}{I_M \sqrt{2\pi \cdot \hat{\beta}}} e^{\left\{ -\frac{[\ln(I_M) - \hat{\mu}]}{2\hat{\beta}^2} \right\}} d(I_M) \tag{3}$$

The median value of A_g for every limit state and the standard deviation are calculated based on the results of nonlinear response-history analysis of all the realizations and different levels of A_g. Their values are obtained from equation 4, where M is the number of realizations and a_i is associated with the onset of collapse for the i^{th} realization [31].

$$\hat{\mu} = \frac{1}{M} \sum_{i=1}^{M} ln(a_i) \tag{4}$$

$$\hat{\beta} = \sqrt{\frac{1}{(M-1)} \sum_{i=1}^{M} (ln(a_i) - \hat{\mu})^2}$$

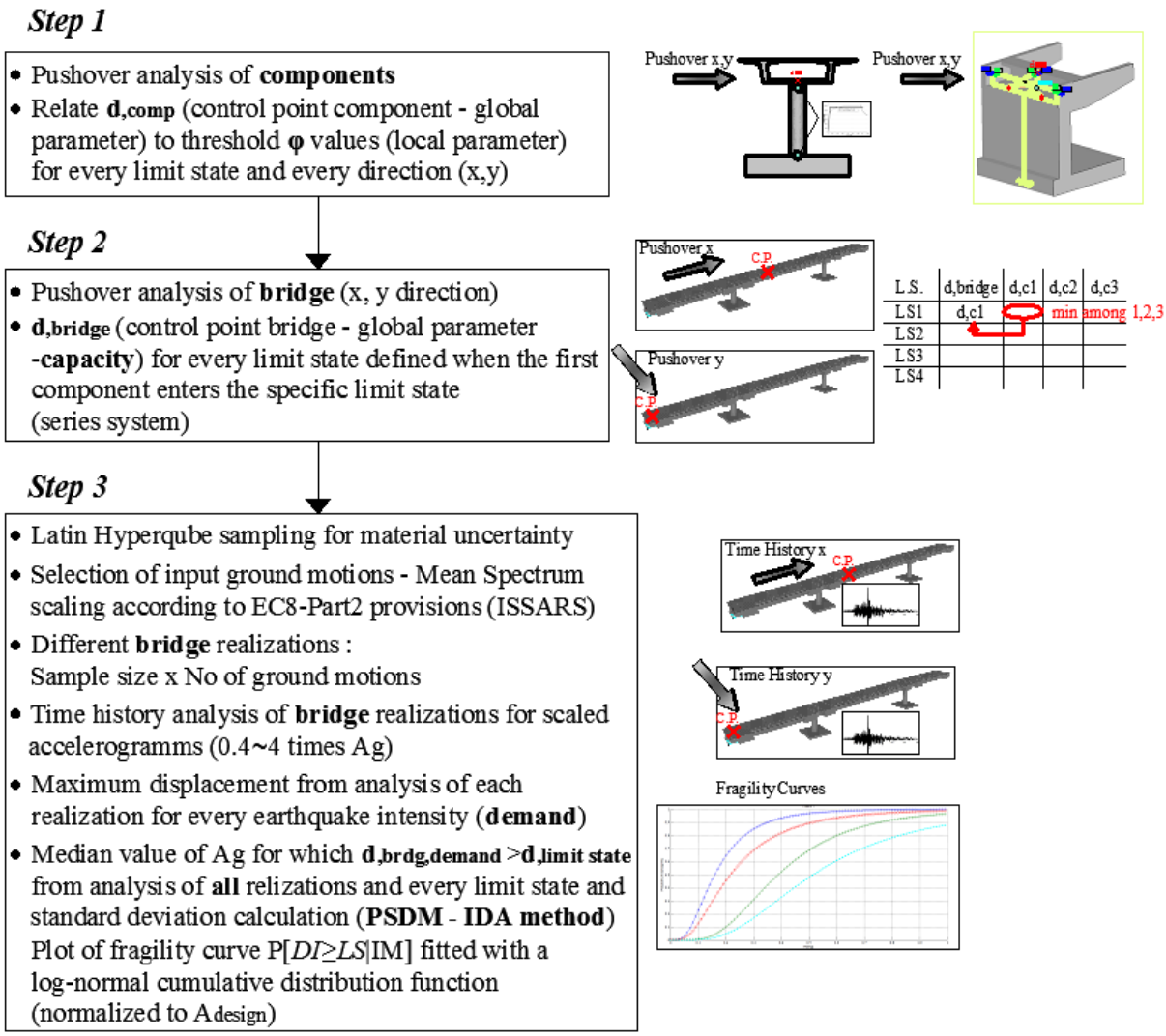

Figure 5: Outline of the proposed methodology.

The methodology presented herein is briefly outlined in Figure 5. It is clear that since, according to the proposed methodology the global capacity is directly related to component performance, it is straightforward to identify the most effective retrofit scheme using the fragility curves for selected performance level(s). A Matlab-code was written for the implementation of the different steps of the methodology.

3 FRAGILITY CURVES OF T7 BRIDGE (AS-BUILT) ACCORDING TO THE PROPOSED METHODOLOGY

The methodology described above is used for the derivation of fragility curves of a case study bridge, a typical overpass of Egnatia Motorway, depicted in Figure 6 and the investigation of the optimum retrofit strategy according to the performance level selected for various seismic events. The two piers having 5.94 m and 7.94 m heights are circular (D=2.0m) and monolithically connected to the deck consisting of a box section. Both piers and abutments have shallow foundations. The deck is connected to the abutment through elastomeric bearings, having a gap in the longitudinal (10 cm) as well as the transverse direction (15 cm).

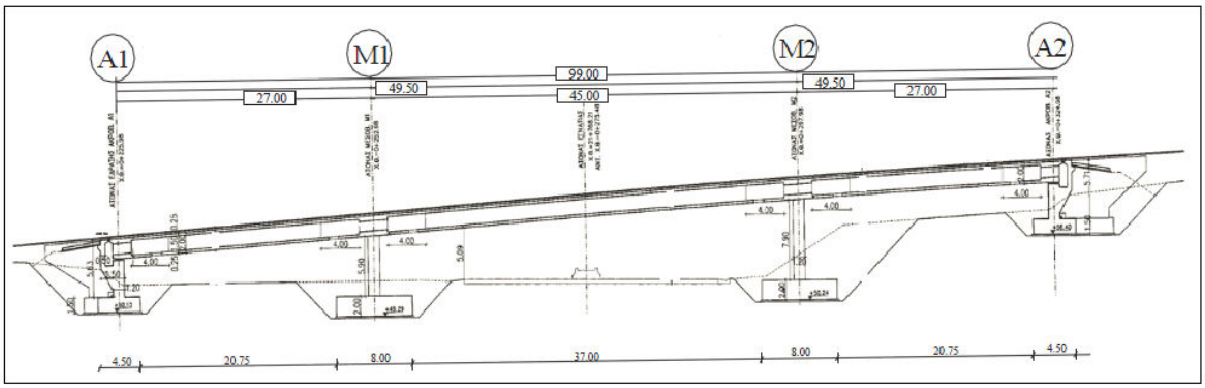

Figure 6: Geometry of T7 Bridge.

3.1 Modelling assumptions

The structure is modelled and analysed using OpenSees [32]. For the formulation of the 3D model as depicted in Figure 7, elastic beam-column elements are used for the deck and beam-column with hinges (lumped plasticity) elements for the piers. Cross section analysis was performed for the piers [23] in order to obtain moment-curvature diagrams for the potential plastic hinges (pier top and bottom), while the plastic hinge length L_p is calculated according to [25]. The abutment-backfill interaction (passive action) after gap closure was considered [22] taking under consideration the relevant Caltrans provisions [33].

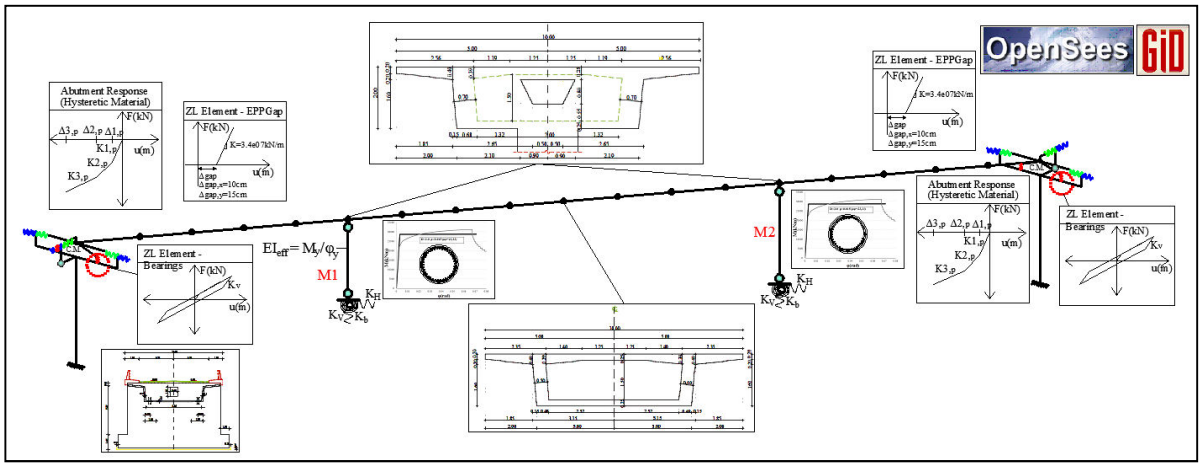

Figure 7: 3D model of T7 overpass bridge.

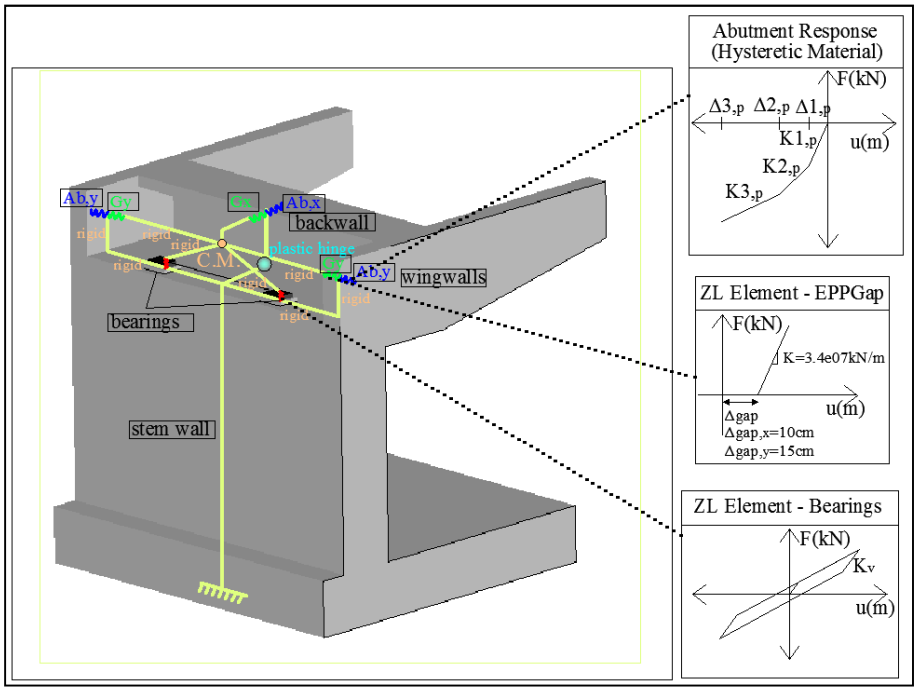

Figure 8: Details of the abutment model.

3.2 Uncertainty treatment

Uncertainty in material properties is considered for the probabilistic assessment of the bridge, regarding concrete compressive strength (f_c) and yield strength of steel (f_y). Concrete and steel strengths are assumed to be a normally distributed random variables, with mean and standard deviation values as shown in Table 4 [9]. The LHS algorithm was employed for N=10 statistically different, yet nominally identical, realizations (resulting to a total number of 700 analyses for the derivation of fragility curves)

Random Variable	Distribution	Mean	Standard deviation
f_c	normal	35.5	3.9
f_y	normal	550	6.13

Table 4: Assumed distributions for random variables.

3.3 Implementation of the methodology (Steps 1 and 2 – System Capacity)

The methodology described is implemented, for the different realizations of the bridge model considered. Pushover analyses (a total of 20) of the components are performed for their longitudinal and the transverse direction (Figure 8), as well as pushover analyses (20) of the bridge system for the two directions.

The most critical component (among piers, abutments, and bearings) defines the threshold value for which the system reaches the specific limit state; this component is generally different for each limit state considered. More specifically, the piers were found to define the first two limit states of the system in both the longitudinal and transverse direction, whereas the bearings through which the bridge deck sits on the abutment the third and fourth ones (corresponding to unseating of the bridge deck). For the bridge type studied here the abutment was not found to define any threshold value for the system, as expected, since gaps of 10 and 15 cm exist between the bridge deck and the abutment in the longitudinal and transverse direction, respectively. However, the abutment interacts with the other components and exceeds the component's threshold limit state values (first and second as depicted in figure 9); this occurs for larger system displacements (subsequent to gap closure), when the other components have already developed excessive deformations and the bridge system is considered to enter a higher limit state.

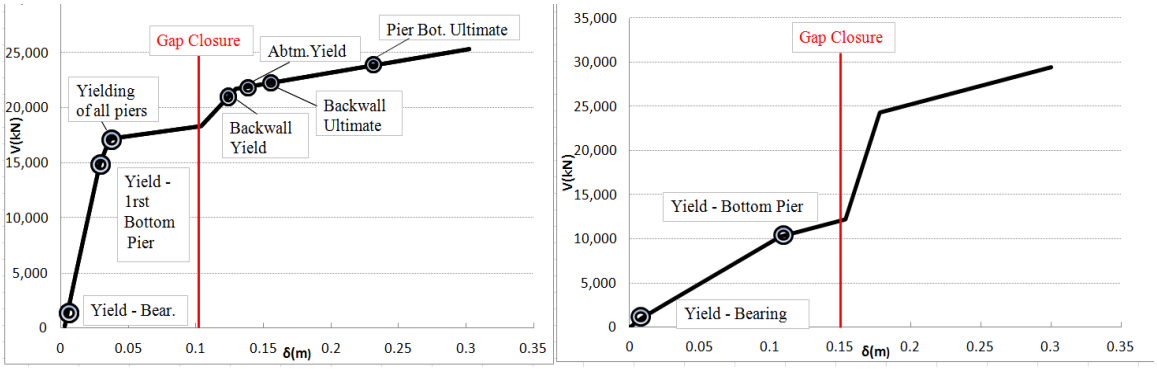

Figure 9: Pushover curves for the bridge's longitudinal (left) and transverse directions.

According to the above, to enhance the system capacity with respect to the first two limit states, retrofit interventions should primarily reduce the vulnerability of the piers, whereas for the last two limit states retrofit measures should focus on increasing the deformation capacity of the bearings and/or reducing the demand to bearings by additional damping. The most efficient retrofit scheme for various seismic intensities according to the prescribed performance level will emerge with the aid of fragility curves, more specifically the comparison between as-built and post-retrofit curves.

3.4 Parametric study of components

In order to investigate the effect of member geometry and reinforcement on the system capacity, a parametric study was carried out for its components, as summarised in Figure 10. The combinations were implemented keeping one parameter constant at a time. Steps 1 and 2 of the proposed methodology were applied, the most critical component for the system derived and subsequently compared with the results for the bridge.

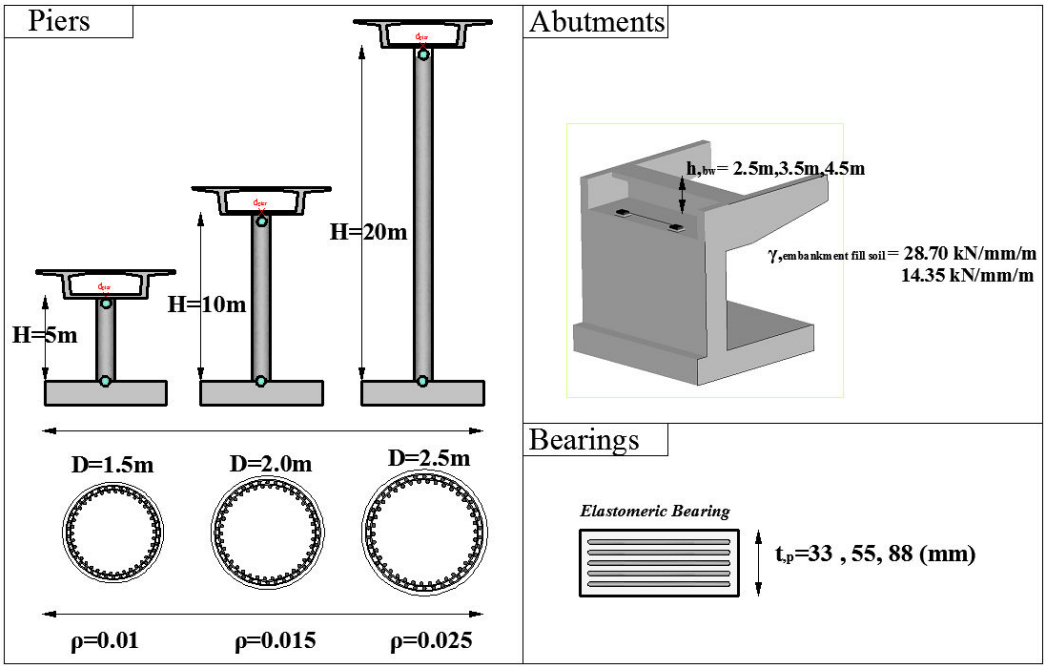

Figure 10: Parametric study of the components of the bridge.

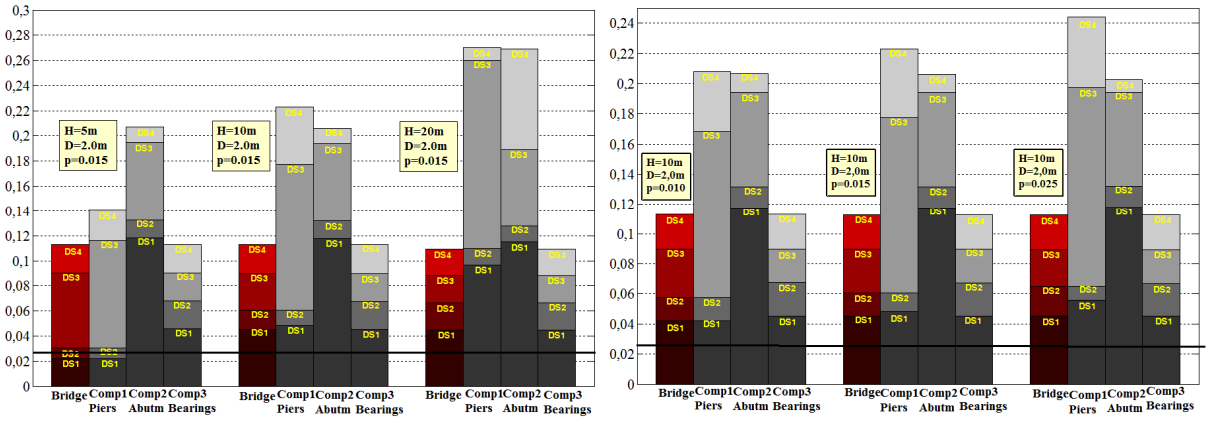

Figure 11: System limit state definition (varying pier height, H, and reinforcement ratio, ρ).

Comparison of the bridge control point displacement when each component exceeds the threshold limit state value is depicted in Figure 11. Threshold values for the system, assuming series connection between the components, are estimated, while the target displacement for the design earthquake is also noted (black line). Therefore the target displacement for the bridge system, calculated for various earthquake intensities, when correlated to the performance level required for the structure (determined by the designer and/or owner) can be directly mapped to the component local performance and guide towards the most efficient retrofit intervention to enhance the seismic performance of the system.

The bridge piers were found to be the most critical component regarding the first two limit states for the majority of cases considered, for both directions (longitudinal and transverse), while the bearings for the two last ones. It is noted that in a few cases, when cohesionless backfill soil was considered, the abutment emerged as more critical than the bearings with regard to the major and collapse limit states. Additionally, when bearings with greater rubber thickness were considered, the piers emerged as the most critical component for all limit states, hence defining the threshold values for the system.

3.5 Derivation of fragility curves (Step 3)

Fragility curves for the T7 bridge (as-built case) are estimated according to the methodology proposed. The 7 accelerograms used for time-history analysis were selected according to Katsanos and Sextos [34] for soil type B and PGA 0.24 and were appropriately scaled according to the EC8-Part 2 provisions [35]. Longitudinal and transverse directions were treated separately (1400 time history analyses – all realizations considered).

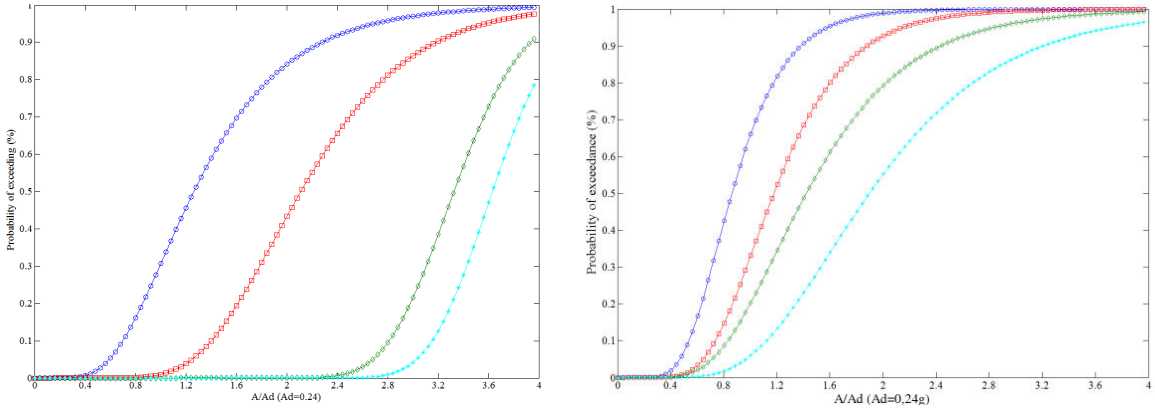

Figure 12: Fragility curves of the as-built bridge: longitudinal (left) and transverse direction.

4 FRAGILITY CURVES OF RETROFITTED BRIDGES AND OPTIMUM SELECTION OF RETROFIT MEASURE

According to the proposed methodology, the most critical member was identified, whose retrofit will efficiently improve the seismic performance of the bridge for the selected performance objective (seismic intensity and associated performance level). However, the most efficient retrofit measures and retrofit strategies for the enhancement of the bridges' seismic performance are not always apparent. In view of this, different retrofit measures and strategies are tested and the optimum strategy solution for the bridge is determined, comparing the as-built and post-retrofit fragility curves.

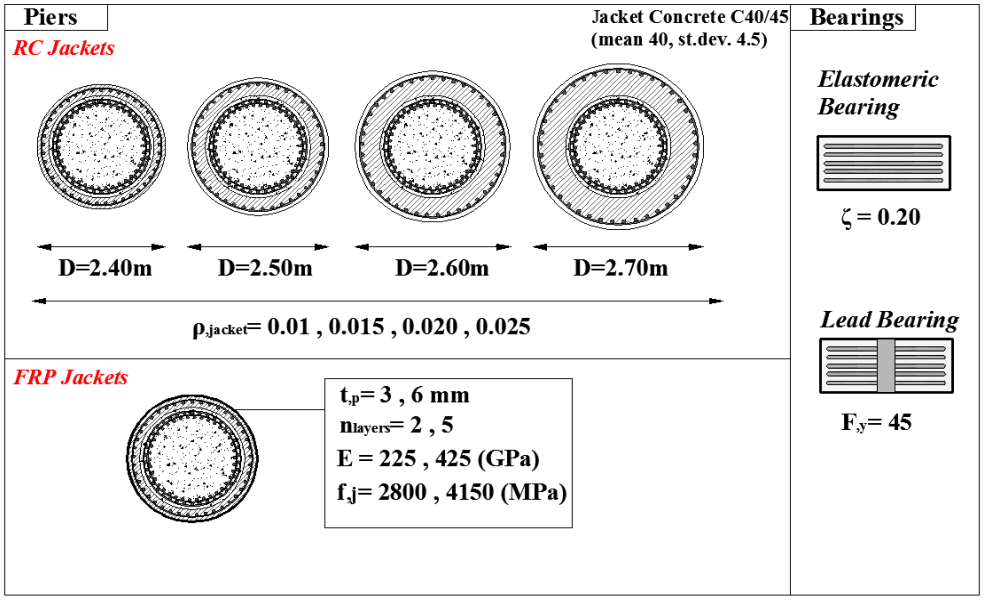

Figure 13: Properties of the retrofit measures considered.

Four different retrofit strategies are examined including R/C and FRP jacketing of the piers and upgrading of the bearings, i.e. use of elastomeric bearings with higher damping, or lead rubber bearings (LRB); different geometric and material properties are considered as depicted in Figure 13.

The proposed methodology is implemented in order to define the retrofitted systems' threshold limit state values and derive the fragility curves. Section analysis for all parameter combinations (16 for the case of R/C jackets and 16 for FRP jackets) are performed in order to derive component threshold values, using appropriate material laws [24, 36].

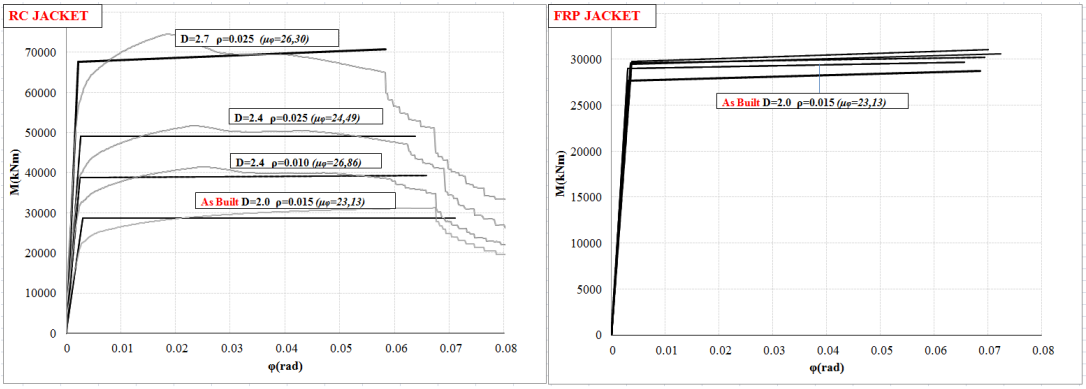

Figure 14: Section analysis of retrofitted structures.

Material uncertainty for the demand and capacity is considered and response-history analyses for the same accelerograms used for fragility analysis of the as-built bridge are performed for all retrofit cases and realizations derived (total number of analyses: 35,000). It is noted that as far as pier retrofit of the as-built bridge is concerned, the same retrofit measure was considered to be implemented to both piers at a time.

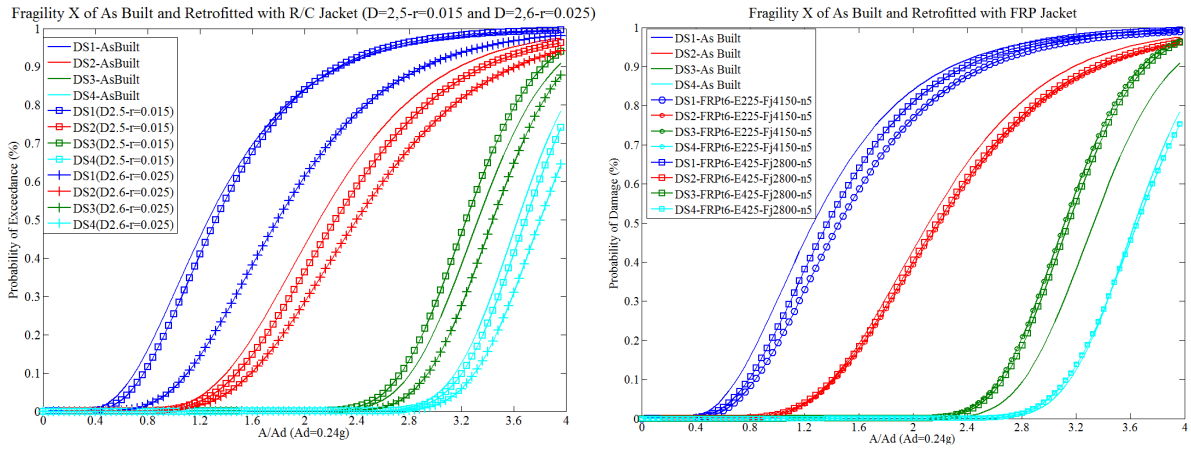

Figure 15: Fragility curves for bridge retrofitted with R/C and FRP jackets compared to as-built case (long.).

Fragility curves for the as-built and retrofitted bridge are compared in Figures 15 and 16 with a view to defining the most effective retrofit measure of the bridge type studied for different performance levels. As shown in Figure 15, retrofitting with R/C jacket obviously enhances the bridge seismic performance as far as the probability of exceedance of the first two limit states (that depend on the pier strength) is concerned, while it has negligible effect on the major and collapse limit state that are mainly controlled by the bearings' performance (recall

the series system assumption). Strengthening of the piers increases the bridge bearing capacity, however it results in higher input seismic forces (increase of stiffness - decrease of the fundamental period) and does not necessarily improve the bridge behaviour. Since the bearings are not replaced or retrofitted, despite the increase in stiffness and strength, the major and collapse limit state are not affected by this retrofit measure. As observed in Figure 15, the effectiveness of this retrofit measure increases for higher reinforcement ratio in the jacket, i.e. as the relative increase in strength exceeds the increase in stiffness, the retrofit measure becomes more effective. Similar conclusions are drawn from the transverse direction assessment (Figure 16-right).

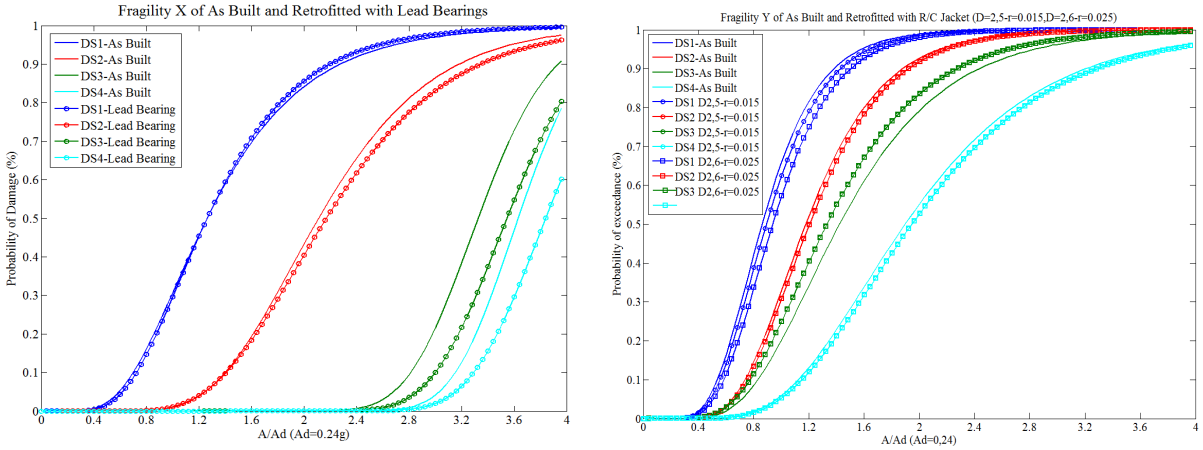

Figure 16: Fragility curves for bridge retrofitted with lead rubber bearings (long) and R/C jackets (trans.) compared to the as-built case.

Retrofitting with FRP jackets also improves the seismic performance for the first two limit states, while it does not affect the performance for the other two. FRP jackets increase pier ductility, nevertheless reaching the last two limit states are controlled by the bearings' performance. Compared to the R/C jacket retrofit, FRPs were found to be less effective for the improvement of the seismic performance for the first two limit states.

Replacement of elastomeric bearings with LRBs with larger rubber thickness was found to be the most effective retrofit measure with respect to major and collapse limit states, while using bearings with higher damping (20%) but the same thickness as the existing bearings was found to have negligible effect on the system's performance.

The aforementioned results refer to the studied bridge type, i.e. bridges with piers monolithically connected to the deck. The different components considered were assumed to be connected in series, a conservative approach that affects the results. It is noted that the studied bridge is a rather recently constructed structure, compliant with existing seismic code provisions; more unfavourable results are expected for non-seismically designed bridges.

5 CONCLUSIONS

In the present study a new methodology for the derivation of fragility curves is presented and implemented to a common type of bridge. The basic aspects of the methodology are the correlation of component limit state threshold values to global ones referring to the whole bridge system and the identification of the most efficient retrofit measure with regard to the selected performance objective(s). Bridge systems with monolithic pier-to-deck connection were assessed for various levels of seismic action and four different retrofit measures were implemented with a view to identifying the most effective one for every limit state, comparing

as-built and post-retrofit fragility curves. An important finding was that different retrofit solutions are the most effective ones, depending on the selected performance level; increasing pier strength (especially by R/C jacketing) improves damage-related performance, whereas increasing the thickness of bearings improves performance related to failure-collapse.

Although combinations of retrofit measures are often used in practice, this study did not evaluate the effect of combinations of retrofit measures on the overall system fragility. Finally, it is noted that for the final selection of the optimum retrofit measure and strategy, the cost of the interventions should also be taken into consideration.

Acknowledgement

This research has been co-financed by the European Union (European Social Fund – ESF) and Greek national funds through the Operational Program "Education and Lifelong Learning" of the National Strategic Reference Framework (NSRF) –Research Funding Program: THALES. Investing in knowledge society through the European Social Fund.

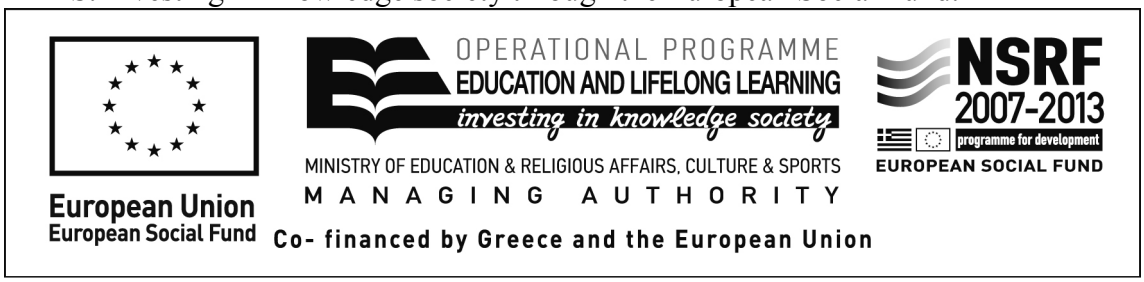

REFERENCES

[1] Y. Zhang, W.F. Cofer, D.I. McLean, Analytical Evaluation of Retrofit Strategies for Multicolumn Bridges, *Journal of Bridge Engineering,* 4(2), 143-150, 1999.

[2] N. Basöz, A.S. Kiremidjian, Evaluation of Bridge Damage Data from the Loma Prieta and Northridge, CA, Earthquakes. *Technical Report* MCEER-98-004, Buffalo, NY, 1998.

[3] Ö. Avşar, A. Yakut, A. Caner, Analytical Fragility Curves for Ordinary Highway Bridges in Turkey. *Earthquake Spectra*, 27(4), 971-996, 2011.

[4] E. Choi, R. DesRoches, B. Nielson, Seismic fragility of typical bridges in moderate seismic zones. *Engineering Structures*, 26(2), 187-199, 2004.

[5] A.S. Elnashai, Borzi B., Vlachos S., Deformation-based vulnerability functions for R/C bridges. *Structural Engineering and Mechanics,* 17(2), 215-244, 2004.

[6] K. R. Karim, F. Yamazaki, F, A simplified method of constructing fragility curves for highway bridges. *Earthquake Engineering & Structural Dynamics*, 32(10), 1603-1626, 2003.

[7] K.R. Mackie, B. Stojadinović, R-Factor Parameterized Bridge Damage Fragility Curves. *Journal of Bridge Engineering*, 12(4), 2007.

[8] I. F. Moschonas, A. J. Kappos, P. Panetsos, V. Papadopoulos, T. Makarios, P. Thanopoulos. Seismic fragility curves for greek bridges: methodology and case studies. *Bulletin of Earthquake Engineering*, 7(2), 439-468, 2008.

[9] B.G. Nielson, R. DesRoches, Seismic fragility methodology for highway bridges using a component level approach, *Earthquake Engineering and Structural Dynamics,* 36, 823-839, 2007.

[10] J.E. Padgett, R. DesRoches, Methodology for the development of analytical fragility curves for retrofitted bridges. *Earthquake Engineering and Structural Dynamics,* 37, 1157-1174, 2008.

[11] J. Zhang, Y. Huo, Evaluating effectiveness and optimum design of isolation devices for highway bridges using the fragility function method. *Engineering Structures,* 31, 1648-1660, 2009.

[12] N. Ataei, J.E. Padgett, Limit state capacities for global performance assessment of bridges exposed to hurricane surge and wave. *Structural Safety,* 41, 73-81, 2013.

[13] K.J. Fridley, Z. Ma, Reliability-based design of seismic retrofit for bridges. *The Washington State Department of Transportation,* Report No. WA-RD 664.1, 2007.

[14] K. Kawashima, Seismic Design and Retrofit of Bridges. *12 World Conference on Earthquake Engineering*, Auckland, New Zealand, Jan. 30-Feb .4, 2000.

[15] B. Binici, Design of FRPs in circular bridge column retrofits for ductility enhancement. *Engineering Structures*, 30(3), 766-776, 2008.

[16] M.F.M. Fahmy, Z. Wu, G. Wu, Post-earthquake recoverability of existing R/C bridge piers retrofitted with FRP composites. *Construction and Building Materials*, 24(6), 980-998, 2009.

[17] R.S. Jangid, Seismic Response of Isolated Bridges. *Journal of Bridge Engineering*, 9(2), 156-166,2004.

[18] J.E. Padgett, Seismic Vulnerability Assessment of Retrofitted Bridges Using Probabilistic Methods, *Ph.D. Thesis,* Georgia Institute of Technology, 2007.

[19] S.-H. Kim, M. Shinozuka, Development of fragility curves of bridges retrofitted by column jacketing. *Probabilistic Engineering Mechanics*, 19(1-2), 105-112, 2004.

[20] V. Bisadi, M. Head, P. Gardoni, Seismic Fragility Estimates and Optimization of Retrofitting Strategies for Reinforced Concrete Bridges: Case Study of the Fabela Bridge in Toluca, Mexico. ASCE *Structures Congress 2011*, 13-22.

[21] B.G. Nielson, Analytical Fragility Curves for Highway Bridges in Moderate Seismic Zones, *Ph.D. Thesis,* Georgia Institute of Technology, 2005.

[22] G. Mylonakis, S. Nikolaou, G. Gazetas, Footings under seismic loading : Analysis and design issues with emphasis on bridge foundations. *Soil Dynamics and Earthquake Engineering*, 26(9), 824-853, 2006.

[23] V.K. Papanikolaou, Analysis of arbitrary composite sections in biaxial bending and axial load. *Computers and Structures*, 98-99, 33-54, 2012.

[24] J.B. Mander, M.J.N. Priestley, R. Park, Theoretical Stress-Strain Model for Confined Concrete. *Journal of Structural Engineering*, 114(8), 1804-1826,1988.

[25] M.J.N. Priestley, G.M. Calvi, M.J. Kowalsky, Displacement-Based Seismic Design of Structures. *IUSS Press, Pavia, Italy*, 2007.

[26] M.N. Sheikh, F. Legeron, Seismic performance-based design of bridges with quantitative local performance criteria, *2nd International Structures Specialty Conference,* June 9-12, Winnipeg, Manitoba, 2010.

[27] F. Naeim, J.M. Kelly, *Design of Seismic Isolated Structures: From Theory to Practice.* John Wiley & Sons, Inc., 1999.

[28] A. Mori, P.J. Moss, N. Cooke, A.J. Carr, The Behavior of Bearings Used for Seismic Isolation under Shear and Axial Load. *Earthquake Spectra,* 15(2), 199-224, 1999.

[29] R.L. Iman, W.J. Conover, A distribution-free approach to inducing rank correlation among input variables. *Communication in Statistics – Simulation and Computation*, 11(3), 311-334, 1982.

[30] C. Dymiotis, A.J. Kappos, M.K. Chryssanthopoulos, Seismic Reliability of R/C Frames with Uncertain Drift and Member Capacity. *Journal of Structural Engineering*, 125(9), 1038-1047 ,1999.

[31] K. Porter, R. Kennedy, R. Bachman, Creating Fragility Functions for Performance-Based Earthquake Engineering. *Earthquake Spectra*, 23(2), 471-489, 2007.

[32] F. McKenna, G.L. Fenves, Open System for Earthquake Engineering Simulation Pacific Earthquake Engineering Research Center, Version 2.4.0., *Pacific Earthquake Research Center,* 2005.

[33] Caltrans, *Caltrans Seismic Design Criteria (2nd end),* California Department of Transportation: Sacramento, CA, 1999.

[34] E.I. Katsanos, A.G. Sextos, ISSARS: An intergrated software environment for structure-specific earthquake ground motion selection. *Advances in Engineering Software*, 58, 70-85, 2013.

[35] CEN (Comité Européen de Normalisation) Eurocode 8 : Design provisions of structures for earthquake resistance - Part 2: Bridges (EN1998-2), CEN Brussels, 2005.

[36] M.R. Spoelstra, G. Monti, FRP-Confined Concrete Model, *Journal of Composites for Construction,* 3, 143-150, 1999.